JOURNAL OF GEOPHYSICAL RESEARCH, VOL. 98, NO. E3, PAGES 5407–5418, MARCH 25, 1993

Kinetics of Crystal Growth in a Terrestrial Magma Ocean

VIATCHESLAV S. SOLOMATOV AND DAVID J. STEVENSON

Division of Geological and Planetary Sciences, California Institute of Technology, Pasadena

The problem of crystal sizes is one of the central problems of differentiation of a terrestrial magma ocean and it has been an arbitrary parameter in previous models. The crystal sizes are controlled by kinetics of nucleation and crystal growth in a convective magma ocean. In contrast with crystallization in magma chambers, volcanic lavas, dikes, and other relatively well studied systems, nucleation and crystallization of solid phases occur due to the adiabatic compression in downward moving magma (adiabatic "cooling"). This problem is solved analytically for an arbitrary crystal growth law, using the following assumptions: convection is not influenced by the kinetics, interface kinetics is the rate controlling mechanism of crystal growth, and the adiabatic cooling is sufficiently slow for the asymptotic solution to be valid. The problems of nucleation and crystal growth at constant heat flux from the system and at constant temperature drop rate are shown to be described with similar equations. This allows comparison with numerical and experimental data available for these cases. A good agreement was found. When, during the cooling, the temperature drops below the temperature of the expected solid phase appearance, the subsequent evolution consists of three basic periods: cooling without any nucleation and crystallization, a short time interval of nucleation and initial crystallization (relaxation to equilibrium), and slow crystallization due to crystal growth controlled by quasi-equilibrium cooling. In contrast to previously discussed problems, nucleation is not as important as the crystal growth rate function and the rate of cooling. The physics of this unusual behavior is that both the characteristic nucleation rate and the time interval during which the nucleation takes place are now controlled by a competition between the cooling and crystallization rates. A probable size range for the magma ocean is found to be $10^{-2} - 1$ cm, which is close to the upper bound for the critical crystal size dividing fractional and nonfractional crystallization discussed elsewhere in this issue. Both the volatile content and pressure are important and can influence the estimate by 1-2 orders of magnitude. Different kinds of Ostwald ripening take place in the final stage of the crystal growth. If the surface nucleation is the rate-controlling mechanism of crystal growth at small supercooling, then the Ostwald ripening is negligibly slow. In the case of other mechanisms of crystal growth, the crystal radius can reach the critical value required to start the fractional crystallization. It can happen in the latest stages of the evolution when the crystals do not dissolve completely and the time for the ripening is large.

INTRODUCTION

Elsewhere [*Solomatov and Stevenson*, this issue (*a*), (*b*)] it has been found that the differentiation of a terrestrial magma ocean strongly depends on the crystal sizes. The crystal sizes cannot be estimated just from the observed surface rocks: it is well-known that the crystal sizes can vary from microscopic sizes of the order of several molecular thicknesses ($10^{-7} - 10^{-6}$ cm) to the largest observed sizes ($1 - 10$ cm), depending on the cooling history. In this paper we make a first step in this problem to determine the crystal sizes in the convective magma ocean.

General Description of the Problem

A simplified picture of the magma ocean [*Solomatov and Stevenson*, this issue (*a*), (*b*)] and the processes of nucleation and crystal growth follow. The total depth of the magma ocean can be $1000 - 3000$ km. The heat flux of $10^6 - 10^9$ ergs cm^{-2} s^{-1} is mostly due to the cooling of the magma ocean and is controlled by the atmosphere covering the magma ocean. The convection is very strong and turbulent. The convective velocities are about 10^2 cm s^{-1}. The presence of crystals has two possible consequences: fractional crystallization when the magma ocean cannot suspend crystals even at small crystal fractions, and nonfractional crystallization when the convection is strong enough to prevent any differentiation. The switch between these two cases is probably determined by the energetics of convection and is sharply defined compared with uncertainties in other parameters such as the boundary conditions determining the heat flux or crystal sizes determining the settling velocity and dissipational heating. In the case of nonfractional crystallization, differentiation eventually occurs in a solid matrix with percolating melt. The crystal size determines the degree of differentiation in this regime because it influences the competition between the percolation rate and the rate of solidification. The crystal size is also an important factor for the problems of nonequilibrium thermodynamics and rheology. For investigation of nonfractional crystallization, it is sufficient to assume here that differentiation is negligible and the magma ocean is chemically uniform.

The temperature of the magma ocean approximately follows a two-phase adiabat of the multicomponent system considered. In the simplest general case, when this adiabat passes through all the depths, it passes through a completely molten uppermost layer, then through a layer containing only the first solid phase, then a layer where the second solid phase enters the melt, and so on. Eventually, the adiabat reaches a completely solid region, though this region may be absent in the beginning of the evolution. The depth interval through which the adiabat follows from the liquidus to solidus is comparable with the magma ocean thickness, and thus each layer occupies a significant portion of the magma ocean.

Paper number 92JE02839.
0148-0227/93/92JE-02839$05.00

Nucleation and crystal growth are controlled not by the entire magma ocean cooling rate (as it would be, for example, in a conductive layer), but by the circulation rate of the fluid between layers where the crystals appear and disappear. Consequently, the nucleation and crystallization are cyclic processes which take place in quasi-steady conditions.

The final crystal size is influenced by Ostwald ripening, which takes place when the crystals circulate in regions of their stability When the crystals have no possibility to dissolve completely, it can be a dominant process. This case is possible during the latest stages of the evolution, when the completely molten layer is absent and the temperature is below the liquidus (or subsequent phase boundaries) everywhere.

Qualitative Analysis of Nucleation and Crystal Growth

Figure 1 shows a cartoon of the magma ocean with an exaggerated scale. Figure 2 shows schematically the temperature variation in a fluid parcel moving down across the nucleation boundary. Before the intersection, the temperature is higher than the temperature for the appearance of the expected solid phase. After the intersection, the supercooling in the moving parcel begins to grow. It will be shown later that the crystallization occurs in a way similar to the crystallization at constant pressure when the temperature drop rate is constant and when the heat loss rate is constant. However, in the problem considered, the supercooling increases due to the difference in slopes between the adiabatic temperature of the moving melt and the slope of the boundary of the solid phase appearance.

Eventually, the supercooling reaches a sufficiently high value, and nucleation and crystallization begin. This process is avalanchelike, and the system quickly reaches almost complete equilibrium. After this, the nucleation mostly ceases, and further motion (or cooling in the constant pressure analog) causes an increase in the crystal fraction due to the crystal growth alone.

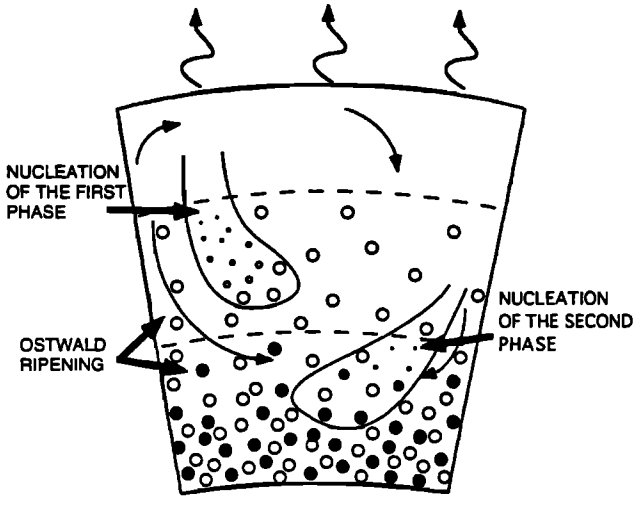

Fig. 1. A schematic cartoon of nucleation and crystallization in a convective magma ocean. The first solid phase nucleates and crystallizes at a depth level where the temperature of a downward moving melt drops below the liquidus (where the adiabat intersects the liquidus). The second and subsequent solid phases nucleate and crystallize when the temperature of the moving fluid (following the adiabats) becomes smaller than the corresponding temperature for the appearance of these solid phases. The cartoon is shown for the case when the liquidus and subsequent phase boundaries are steeper than the adiabats [*Solomatov and Stevenson*, this issue (*b*)].

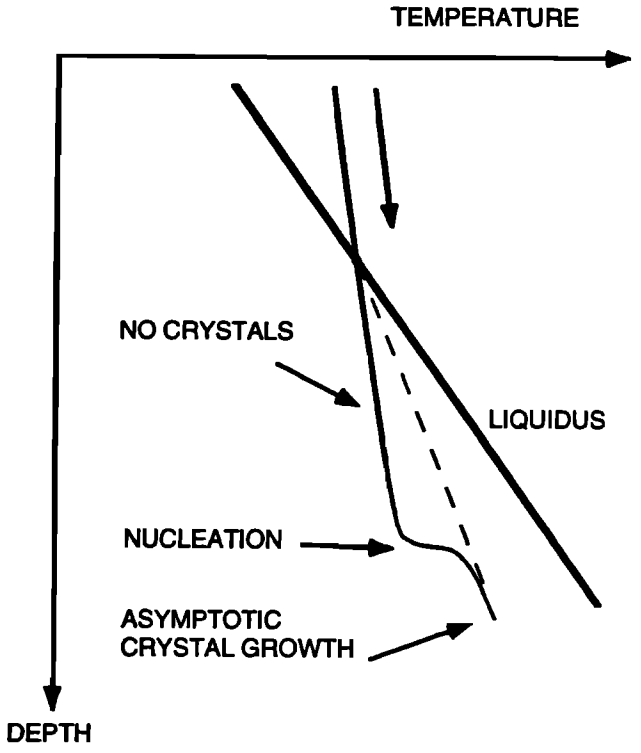

Fig. 2. Temperature changes and nucleation and crystallization in a fluid parcel passing the liquidus (heavy solid line). The real temperature of the fluid parcel (solid line) is a pure melt adiabat before and just after the liquidus (in the metastable region). The temperature asymptotically approaches the equilibrium adiabat in the two-phase region (dashed line) after a short period of nucleation. The arrow shows the direction of motion.

In the case of very high cooling rates, the cooling without nucleation can reach even the solidus temperature. This case is very different from the one considered: the subsequent order of solid phases can be changed, glass can be produced, and the mathematical analysis is different. As will be clear from the quantitative considerations, this is an impossible case for the magma ocean because of slow cooling rates ($10^{-4} - 10^{-3}$ K s^{-1}) and small maximum supercooling ($10 - 30$ K), and it is not considered here.

Composition and Multi-Component Thermodynamics of Partial Melts

Because the magma ocean is considered as a molten undepleted mantle, the composition of magma corresponds to the bulk composition of the mantle (after core formation). A simple model for this system is developed by *Solomatov and Stevenson* [this issue (*b*)] which allows calculation of all equilibrium thermodynamical parameters in the entire melting range. The model consists of three components which form a eutecticlike system or a system where two components produce a solid solution. Both models are ideal but give a reasonable agreement with experimental data and can work as a basis for the consideration of the nucleation and crystal growth. The first liquidus phase is olivine ($P < 15$ GPa), garnet considered as a solid solution ($15 < P < 25$ GPa), perovskite ($P > 25$ GPa), and possibly magnesiowüstite (considered as a solid solution between MgO and FeO) which

can substitute for perovskite at higher pressures. The crystal sizes of the first liquidus phases are mostly important because the competition between convection and settling is crucial at small crystal fractions [*Solomatov and Stevenson*, this issue (*a*), (*b*)] However, the model is developed also for the nucleation and crystallization of the second and subsequent phases. In this case, we assume that before the formation of a new phase, the subsystem consisting of the melt and the existing solid phases is close to its equilibrium. This subsystem is described in terms of the multiphase equilibrium thermodynamics [*Solomatov and Stevenson*, this issue (*b*)], and the problem of the second phase formation (in a nonstep melting case) is mathematically similar to the first liquidus phase formation (see details below).

Difference From Magma Chambers

A small-scale analog to magma oceans is magma chambers, fluid dynamics and crystallization, which are relatively studied [see, e.g., *Sparks et al.*, 1984; *Huppert and Sparks*, 1984; *Martin et al.*, 1987; *Marsh*, 1987, 1988*a*,*b*, 1989*a*,*b*, *Martin*, 1990; *Worster et al.*, 1990]. However, deep magma oceans are different in many ways. As a most pronounced example is that nonfractional style of crystallization assumed in this paper and studied by *Solomatov and Stevenson*, this issue (*a*), (*b*)] is impossible at depths less than 100 − 300 km and thus is irrelevant to magma chambers (< 1 − 10 km). The nucleation and crystallization are due to adiabatic compression in downward convective flows or, in some pressure ranges, due to adiabatic decompression in upward flows. This kind of internal nucleation and crystallization might be relevant to magma chambers, but the presence of a solid lid, floor and walls is believed to be a more important factor. Crystallization in the surface thermal boundary layers in the magma ocean is followed by melting due to equilibrating with the potential temperature upon exit from the boundary layers and has no direct influence on the crystal growth. Solid boundaries and walls are absent and cannot be the places for nucleation and crystal growth. Even the floor in the common sense is absent; the crystal fraction increases continuously with depth. The composition of the chondritelike or peridotitelike magma ocean is also different from a basaltic composition of the magma chambers.

Nucleation and Crystal Growth

We follow a common physics of nucleation and crystal growth which is discussed in many works [e.g., *Dunning*, 1969; *Lifshits and Pitaevskii*, 1981; *Dowty*, 1980; *Kirkpatrick*, 1981; *Randolph and Larson*, 1988]. We consider a problem where cooling starts well above the liquidus or above the temperature for the appearance of the solid phase considered. Although this could imply the homogeneous nucleation, usually a heterogeneous nucleation dominates due to various imperfections. Moreover, when the second and subsequent solid phases are considered, the nucleation is likely to be heterogeneous, because the preexisting crystals of other solid phases can be sites of preferable nucleation [*Lofgren*, 1983, 1989; *Hort and Spohn*, 1991*a*]. We describe the heterogeneous nucleation by choosing a reduced value for the surface tension [*Dowty*, 1980; *Lofgren*, 1983].

One of the specific features of silicate systems is that the mechanisms of crystal growth vary with composition. We find an analytical solution for any arbitrary mechanism of interface kinetics controlled crystal growth.

Previous Laboratory and Numerical Experiments

The problem has two, almost exact, constant pressure analogs: the cooling at constant heat loss rate and at constant temperature drop rate. This fact allows comparison with corresponding numerical and experimental data which provide the dependence of the crystal sizes on the cooling rate. The experimental data were selected on the basis of the following requirements. The initial temperature must be higher than the temperature for the appearance of the solid phase studied (in the magma ocean case it is higher by hundreds of kelvins during most of the evolution). In the opposite case, the preexisting crystals of the solidifying phase influence the crystallization conditions [*Walker et al.*, 1978; *Lofgren*, 1983, 1989; *Grove*, 1990] (see also discussion section). The cooling rate must be constant and not be influenced by the thermal diffusion as in the field experiments [see, e.g., *Ikeda*, 1977] where the cooling rate is changing with time. This makes the problem different from the problem considered which does not involve any thermal diffusion process.

A serious problem is that the experimental data for all magma ocean liquidus phases are absent. So, the data are used to test the theory and then the theory is used to predict crystal sizes for the magma ocean liquidus phases.

The relevant experimental data which are used for comparison with the theory are from *Lofgren et al.* [1974], *Grove* [1978], *Walker et al.* [1978], and *Grove and Walker* [1977]. The numerical data are from *Dowty* [1980]. *Toramaru* [1991] also considered this problem numerically, but for the case when the compositional diffusion is the rate controlling factor. The same problem was recently studied by *Hort and Spohn* [1991*b*] where, however, the emphasis is on the transition between slowly and rapidly cooling regimes but not on the dependences of the crystal sizes on the cooling rate.

Previous Analytical Results

The previous analytical calculations or scaling analysis considered nucleation and crystallization in different conditions: isothermal crystallization, initially supercooled and thermally isolated systems, various problems of crystallization controlled by thermal diffusion, and rapidly quenched systems [see, e.g., *Avrami*, 1939, 1941; *Christian*, 1965; *Brandeis and Jaupart*, 1986, 1987; *Brandeis et al.*, 1984; *Buyevich and Mansurov*, 1990] However, there is no analytical solution or scaling law for the slowly cooling systems. We will show that the solution for the problem considered is quite different from the other problems and has different controlling parameters.

THE MODEL

Consider the Lagrangian reference scheme attached to a small fluid parcel. Motion of this fluid parcel in the internal region of a laminar or turbulent convective magma ocean is almost adiabatic. When the fluid parcel moves from lower pressure regions to higher pressure regions, the equilibrium temperature of the fluid parcel changes in accordance with the adiabats calculated by *Solomatov and Stevenson* [this issue (*b*)]. In passing a phase boundary, the correspondent solid phase appears and reaches equilibrium, not instantly, but after a period of supercooling during which nucleation and crystal growth take place. The slope of the adiabat also changes, not instantly, but during this nonequilibrium

regime. The assumptions which will be used are the following: (1) there is complete thermodynamical equilibrium for other solid phases if they are present in the system, (2) thermal diffusion is the fastest kinetic process, and thus after the intersection, the phase boundary there is a local thermal equilibrium. Now in contrast to the complete equilibrium thermodynamics considered by *Solomatov and Stevenson* [this issue (*b*)], we have three thermodynamical parameters: temperature T, pressure p, and the crystal fraction of the new phase ϕ (any dependence on kinetically induced nonequilibrium compositional changes is ignored). The last parameter is now controlled by kinetic equations.

Before the phase boundary is encounted, the rate of the entropy change for the fluid parcel is equal to 0 (ignoring a small irreversible entropy production):

$$\frac{ds}{dt} = \left(\frac{\partial s}{\partial T}\right)_p^{(1)} \left(\frac{dT}{dt}\right)^{(1)} + \left(\frac{\partial s}{\partial p}\right)_T^{(1)} \left(\frac{dp}{dt}\right)^{(1)} = 0, \quad (1)$$

where the superscript "1" means the thermodynamical parameters per unit mass before the phase boundary.

After the phase boundary,

$$\frac{ds}{dt} = \left(\frac{\partial s}{\partial T}\right)_{p,\phi}^{(2)} \left(\frac{dT}{dt}\right)^{(2)} + \left(\frac{\partial s}{\partial p}\right)_{T,\phi}^{(2)} \left(\frac{dp}{dt}\right)^{(2)} + \left(\frac{\partial s}{\partial \phi}\right)_{p,T}^{(2)} \left(\frac{d\phi}{dt}\right)^{(2)} = 0, \quad (2)$$

where the superscript "2" means the thermodynamical parameters per unit mass after the phase boundary.

The thermodynamical parameters after the phase boundary calculated at $\phi = \text{const}$ are approximately equal to the thermodynamical parameters before the phase boundary:

$$\left(\frac{\partial s}{\partial T}\right)_{p,\phi}^{(2)} \approx \left(\frac{\partial s}{\partial T}\right)_p^{(1)}, \quad \left(\frac{\partial s}{\partial p}\right)_{T,\phi}^{(2)} \approx \left(\frac{\partial s}{\partial p}\right)_T^{(1)}. \quad (3)$$

We also suppose that the characteristic convective velocity before and after the phase boundary is the same and can be taken as a constant and thus

$$\left(\frac{dp}{dt}\right)^{(1)} \approx \left(\frac{dp}{dt}\right)^{(2)} \approx \frac{dp}{dz} v_{\text{conv}}. \quad (4)$$

The equilibrium temperature $T_e(p, \phi)$ is equal to the current liquidus temperature of the melt and depends on the chemical composition of the melt or, in an ideal case, on the current crystal fraction:

$$\frac{dT_e}{dt} = \left(\frac{\partial T_e}{\partial p}\right)_\phi \frac{dp}{dt} + \left(\frac{\partial T_e}{\partial \phi}\right)_p \frac{d\phi}{dt}. \quad (5)$$

Introducing the supercooling

$$T' = T'(t) = T_e - T > 0 \quad (6)$$

we write

$$\frac{dT'}{dt} = \left[\left(\frac{\partial T_e}{\partial p}\right)_\phi + \frac{(\partial s/\partial p)_{T,\phi}}{(\partial s/\partial T)_{p,\phi}}\right] \frac{dp}{dt} + \left[\left(\frac{\partial T_e}{\partial \phi}\right)_p + \frac{(\partial s/\partial \phi)_{T,p}}{(\partial s/\partial T)_{p,\phi}}\right] \frac{d\phi}{dt}. \quad (7)$$

With sufficient accuracy, the above equation can be rewritten as

$$\frac{dT'}{dt} = -\frac{\Delta H}{c_p^{(1)}} \frac{d\phi}{dt} + \frac{d(T_{\text{ph}} - T_{\text{ad}}^{(1)})}{dz} v_{\text{conv}}, \quad (8)$$

where dT_{ph}/dz is the phase boundary slope, $dT_{\text{ad}}^{(1)}/dz$ is the equilibrium adiabatic temperature gradient before the phase boundary, v_{conv} is a characteristic convective velocity, ΔH is the enthalpy change on melting, and $c_p^{(1)}$ is the thermal capacity at constant pressure per unit mass of the system before the phase boundary. The ratio

$$\frac{(\partial T_e/\partial \phi)_p}{\Delta H/c_p^{(1)}} \sim \frac{c_p^{(1)}}{c_p^{(2)}} \ll 1 \quad (9)$$

was ignored (although it is not an essential assumption), because it is usually small [*Solomatov and Stevenson*, this issue (*b*)], where $c_p^{(2)}$ is the equilibrium multiphase thermal capacity after the phase boundary.

The function $d\phi/dt$ is expressed as follows [*Randolph and Larson*, 1988]:

$$\frac{d\phi}{dt} = \int_0^\infty 4\pi r^2 G(T', r) f(r, t) dr \quad (10)$$

where for simplicity, we ignore the difference between the volume and mass fraction of the new phase, r is the crystal radius, and $f(r, t)$ is the function of crystal size distribution. The value $f(r, t)dr$ is equal to the number of crystals between r and $r + dr$ per unit volume, so that

$$\int_0^\infty f(r, t) dr = N, \quad (11)$$

N is the number of crystals per unit volume. The linear crystal growth rate $G(T', r) = dr/dt$ depends on the mechanisms of crystal growth. The kinetic processes at the crystal surface dominate when the crystal size is small. The diffusion rate decreases with increasing crystal radius, and eventually at some large crystal radius, the compositional or thermal diffusion becomes the rate-controlling process. For the silicate systems, interface kinetics is usually the slowest process even for typical (fully grown) crystal sizes, and we will suppose that the interface kinetics is the rate-controlling mechanism of crystal growth [*Kirkpatrick*, 1975, 1981; *Dowty*, 1980]. If so, the function $G(T', r)$ depends only on the supercooling:

$$G(T', r) \approx G(T'). \quad (12)$$

The continuity equation is [*Randolph and Larson*, 1988]

$$\frac{\partial f}{\partial t} + \frac{\partial (Gf)}{\partial r} = \frac{\partial f}{\partial t} + G\frac{\partial f}{\partial r} = 0. \quad (13)$$

The boundary condition at $r = 0$ is

$$G(T') f(0, t) = J(T') \quad (14)$$

where $J(T')$ is the nucleation rate (number of nuclei per unit time per unit volume). The function for the nucleation rate is [*Dunning*, 1969; *Kirkpatrick*, 1975, 1981; *Dowty*, 1980; *Lifshitz and Pitaevskii*, 1981]

$$J(T') = a \exp\left(-\frac{A}{T'^2}\right), \quad (15)$$

where a and A are approximately constants.

The initial conditions at the time $t = 0$ when the fluid parcel has just past the phase boundary are

$$f(r, 0) = 0, \quad T'(0) = 0. \quad (16)$$

The solution to the above equations is given in the appendix.

SIMILARITY BETWEEN DIFFERENT KINETIC PROBLEMS

The direct experimental data for the problem considered are obviously absent. However, there are experimental and numerical data for the two problems of crystallization: at constant temperature drop rate and at constant heat loss rate. We show below that the mathematical formulations for these problems are exactly the same as for the problem considered except that the definitions of the constants are different.

The heat balance equation for both problems is

$$c_p^{(1)}\frac{dT}{dt} = \Delta H\frac{d\phi}{dt} - Q_0, \tag{17}$$

where $Q_0 > 0$ is the heat loss rate.

The current equilibrium temperature T_e corresponding to the current crystal fraction ϕ is determined by the equation

$$\frac{dT_e(\phi(t))}{dt} = \frac{dT_e(\phi)}{d\phi}\frac{d\phi}{dt}. \tag{18}$$

In terms of $c_p^{(1)}$ and $c_p^{(2)}$ the derivative $dT_e(\phi)/d\phi$ is written as

$$\frac{dT_e(\phi)}{d\phi} = -\frac{\Delta H}{c_p^{(2)} - c_p^{(1)}} \tag{19}$$

and (17) becomes as follows:

$$\frac{dT'}{dt} = -\frac{\Delta H}{c_p^{(1)}}\frac{c_p^{(2)}}{c_p^{(2)} - c_p^{(1)}}\frac{d\phi}{dt} + \frac{Q_0}{c_p^{(1)}} \approx -\frac{\Delta H}{c_p^{(1)}}\frac{d\phi}{dt} + \frac{Q_0}{c_p^{(1)}}, \tag{20}$$

where $T' = T_e - T$ is the supercooling.

If the temperature drop rate $\dot{T}_0 = -dT/dt > 0$ is constant, then we have

$$\frac{dT'}{dt} = -\frac{\Delta H}{c_p^{(2)} - c_p^{(1)}}\frac{d\phi}{dt} + \dot{T}_0 \approx -\frac{\Delta H}{c_p^{(2)}}\frac{d\phi}{dt} + \dot{T}_0. \tag{21}$$

The heat balance equations for the crystallization in adiabatic cooling (8), at constant heat loss rate (20), and at constant temperature drop rate (21) are essentially similar. The continuity equation and boundary and initial conditions are kept without any changes.

The averaged radius r_∞ of crystals (spheres) on crystallization of the solid phase considered is found from the solution to these problems as follows (see appendix, (92), (93), (96)). The maximum (dimensional) supercooling reached during cooling is

$$T'_m = \left(\frac{A}{p}\right)^{1/2}, \tag{22}$$

where the nondimensional parameter p is found from the transcendental equation

$$p = \ln\left[\frac{\pi^3\Delta H a A^{3/2} G_m^3}{2^6 c_p^{(i)}\dot{T}^4 p^{9/2}}\right]. \tag{23}$$

The crystal growth rate at this supercooling is

$$G_m = G(T')\big|_{T'=(A/p)^{1/2}}, \tag{24}$$

the number of crystals per unit volume is

$$N = \frac{2^4 c_p^{(i)}\dot{T}^3 p^3}{\pi^2\Delta H A G_m^3}, \tag{25}$$

the final radius is

$$r_\infty = \left(\frac{3\phi_\infty}{4\pi N}\right)^{1/3}. \tag{26}$$

The thermal capacity $c_p^{(i)}$ is

$$c_p^{(i)} = c_p^{(1)}, \tag{27}$$

for adiabatic cooling and constant heat loss rate, and

$$c_p^{(i)} = c_p^{(2)}, \tag{28}$$

for constant temperature drop rate.

The cooling rate $\dot{T}$ is

$$\dot{T} = \frac{d(T_{\rm ph} - T_{\rm ad}^{(1)})}{dz} v_{\rm conv}, \tag{29}$$

for adiabatic cooling,

$$\dot{T} = \frac{Q_0}{c_p^{(1)}}, \tag{30}$$

for constant heat loss rate, and

$$\dot{T} = \dot{T}_0 \tag{31}$$

for constant temperature drop rate.

COMPARISON WITH EXPERIMENTS AND ESTIMATES FOR A MAGMA OCEAN

The parameter found in the experiments is the averaged crystal radius on crystallization. The above equations show that when $p \gg 1$ (very slow cooling), the crystal radius r_∞ is given to logarithmic accuracy by

$$r_\infty \approx \zeta\frac{G_m}{\dot{T}}\left(\frac{\phi_\infty\Delta H A}{c_p^{(i)}}\right)^{1/3}, \tag{32}$$

where $\zeta \sim 10^{-2} - 10^{-1}$ is almost constant. Thus, only two parameters are important: the "external" parameter $\dot{T}$ characterizing the rate of supercooling and the "internal" parameter $G(T')$ characterizing the crystal growth rate.

There are three mechanisms responsible for the crystal growth via interface kinetics [*Kirkpatrick*, 1975, 1981; *Dowty*, 1980; *Randolph and Larson*, 1988]: the continuous growth mechanism where the molecules can be attached to the crystal surface just on reaching it, the screw dislocation mechanism where the molecules are attached to the screw dislocations, and the surface nucleation mechanism which is a two-dimensional analog to the bulk nucleation. We suppose that for the silicate systems considered, the surface nucleation is the main mechanism of crystal growth [e.g, *Dowty*, 1980]. We only note that with other mechanisms, qualitatively similar results are obtained. At small supercooling the function of crystal growth is approximately written as

$$G(T') = b\exp\left(-\frac{B}{T'}\right) \tag{33}$$

and thus

$$G_m = b\exp\left(-\frac{B}{T'_m}\right) = b\exp\left(-\frac{B}{A^{1/2}}p^{1/2}\right), \tag{34}$$

where b and B are constants.

The kinetic parameters can be found from the experimental data for the peak crystal growth rate $G_{\rm peak}$, the supercooling ΔT_G at which this peak takes place, the peak nucleation rate $J_{\rm peak}$, and the supercooling ΔT_J.

The existence of the crystal growth and nucleation peaks is due to the decreasing diffusion rate in the liquid when the supercooling increases and, correspondingly, the absolute temperature drops. The diffusion term is present in both coefficients a and b as

$$\exp\left(-\frac{\Delta H_{\rm diff}}{RT}\right) \approx \exp\left(-\frac{C}{T}\right) \tag{35}$$

where $\Delta H_{\rm diff}$ is the activation enthalpy for the diffusion and $C = \Delta H_{\rm diff}/R$ is a constant. This constant can be estimated from the viscosity measurements supposing that the viscosity is inversely proportional to the diffusion (Einstein's formula): $C \approx 3 \times 10^4$ K [e.g. *Shaw*, 1969]. The experimental data on nucleation and crystal growth in silicate systems suggest similar values [*Dowty*, 1980].

Elementary calculation of the maximums of the functions of nucleation and crystal growth rate gives the following approximate relations:

$$b \approx G_{\rm peak} \exp\left(\frac{(BC)^{1/2}}{T}\right) \approx$$

$$G_{\rm peak} \exp\left(\frac{\Delta T_G C}{T^2}\right) \approx O(1) G_{\rm peak}, \tag{36}$$

$$a \approx J_{\rm peak} \exp\left(\frac{AC^2}{4T^4}\right)^{1/3} \approx$$

$$J_{\rm peak} \exp\left(\frac{\Delta T_J C}{2^{1/3} T^2}\right) \approx O(1) J_{\rm peak}, \tag{37}$$

$$\frac{B}{A^{1/2}} \approx \frac{2^{1/2} \Delta T_G^2 C^{1/2}}{\Delta T_J^{3/2} T} \tag{38}$$

where $O(1) \sim 1$ and thus the coefficients a and b are of the order of the corresponding peak values. The significance of this result is that we can use available experimental data on both peaks to estimate the parameters b and $B/A^{1/2}$. Substituting, for example, some typical values $\Delta T_G = 30$ K and $\Delta T_J = 100$ K (see data in *Dowty* [1980]), we obtain $B/A^{1/2} \approx 0.5$. However, it is known that a formal approach can significantly underestimate the coefficient a in the nucleation rate function (probably by 14 and even more orders of magnitude [*Kirkpatrick*, 1981]).

The theoretical expressions for $A^{1/2}$ and B give some independent estimates for $B/A^{1/2}$:

$$A^{1/2} = \left(\frac{16\pi\sigma^3 T}{3k_B(\rho\Delta H)^2}\right)^{1/2} \sim 100 \text{ K}, \tag{39}$$

$$B = \frac{\pi\sigma^2 d_n}{k_B \Delta H^2} \sim 30 \text{ K}, \tag{40}$$

and thus

$$\frac{B}{A^{1/2}} \approx 0.3, \tag{41}$$

where $\sigma \approx 20$ ergs cm^{-2} is a reduced surface tension for nucleation [*Dowty*, 1980], $T \approx 1000$ K is the temperature, $k_B \approx 1.4 \times 10^{-16}$ ergs K^{-1} is Boltzmann's constant, $\rho \approx 3$ g cm^{-3} is the density, $\Delta H \approx 3 \times 10^9$ ergs g^{-1} is the enthalpy change on melting, and $d_n \approx 3 \times 10^{-8}$ cm is the thickness of the surface nuclei. For large crystals, B can be reduced by a factor of 3, but this is less certain. For a homogeneous nucleation, the effective surface tension is closer to its normal value. In such a case, the estimate for $B/A^{1/2}$ would be a few times larger.

In the calculations, the parameters b, $B/A^{1/2}$ and also a were varied. The parameter A was taken as 10^4 K^2. The thermal capacity at constant pressure is about $c_p \approx 10^7$ ergs g^{-1} K^{-1}. The effective thermal capacity $c_p^{(2)}$ in the problem with constant temperature drop rate can be ~ 1 order of magnitude larger than the "normal" thermal capacity, but the correspondent change in the crystal radius is only $(c_p^{(1)}/c_p^{(2)})^{1/3} \approx 0.5$.

The theoretical curves together with some experimental and numerical data are shown in Figure 3. The fit can be done with different sets of the parameters. The estimates are very sensitive to the parameter $b \sim G_{\rm peak}$ and thus, it is the minimum information needed for a rough estimate, if the cooling rate is known. As it is seen from Figure 3, plagioclase crystals are smaller than the diopside crystals by approximately one order of magnitude at the same cooling rate. This could be due to different factors: b is smaller by one order of magnitude, $B/A^{1/2}$ is about 4 times higher, or a is about 15 orders of magnitude larger (although these

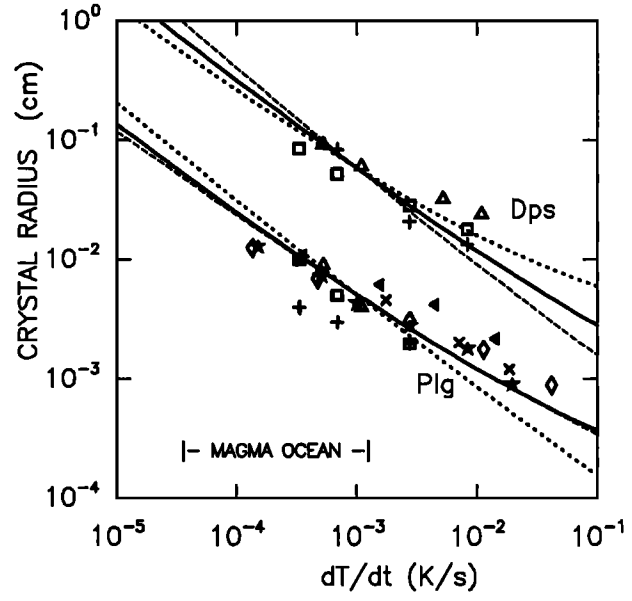

Fig. 3. Analytical and experimental dependences of the crystal radius on the parameter $\dot{T}$ discussed in the text. The data are collected by *Dowty* [1980] and by *Cashman* [1992]. Experimental data are for the constant temperature drop rate: crosses, *Lofgren et al.* [1974] (for plagioclase and for diopside in the system Di–Ab–An); diamond, *Grove* [1978]; solid triangles, *Walker et al.* [1978] ($T(0) = 1155^{\rm O}$ C); X's, *Walker et al.* [1978] ($T(0) = 1200^{\rm O}$ C); stars, *Grove and Walker* [1977]. Numerical modeling by *Dowty* [1980] (for plagioclase and for diopside in the system Di–Ab–An): squares, constant temperature drop rate; open triangles, constant heat loss rate. The theoretical curves fit the data with the help of different sets of b, a, and $\zeta = B/A^{1/2}$. At the same cooling rate, the difference between diopside and plagioclase crystal sizes can be equally explained by an order of magnitude difference in b (solid lines, $b_{\rm dps} = 2.4 \times 10^{-4}$ cm s^{-1}, $b_{\rm plg} = 1.0 \times 10^{-5}$ cm s^{-1}, and, for both minerals, $a = 8.3 \times 10^9$ cm^{-3} s^{-1} and $\zeta = 0.5$), or by 15 orders of magnitude difference in a (dotted lines, $a_{\rm dps} = 7.6 \times 10^4$ cm^{-3} s^{-1}, $a_{\rm plg} = 1.0 \times 10^{20}$ cm^{-3} s^{-1}, and, for both minerals, $\zeta = 0.5$, $b = 7.0 \times 10^{-5}$ cm s^{-1}), or by a 4 times difference in $\zeta = B/A^{1/2}$ (dashed lines, $\zeta_{\rm dps} = 0.2$, $\zeta_{\rm plg} = 0.8$, and, for both minerals, $b = 8.4 \times 10^{-5}$ cm s^{-1} and $a = 7.2 \times 10^{12}$ cm^{-3}s^{-1}). A possible range of $\dot{T}$ for the magma ocean is shown.

estimates depend on the parameter range considered). The crystal size is sensitive mostly to the first two factors. The simplest explanation is that the viscosity of melt during crystallization of plagioclase was higher. Thus, the parameter b (which is proportional to the diffusion coefficient and inversely proportional to the viscosity) can be smaller for the plagioclase. For the silicate systems, the typical values of the peak crystal growth rate are $10^{-5}-10^{-4}$ cm s^{-1} [*Dowty*, 1980], that is close to the values of $b \sim G_{\text{peak}}$ predicted by the model (Figure 3). The influence of the parameter a seems to be less important. However, parameter a is proportional to the number of sites available for heterogeneous nucleation, and thus a significant increase in a is possible in the case of plagioclase, because of the presence of diopside crystals crystallized earlier.

To estimate the crystal sizes in the magma ocean, we need at least the value of the peak crystal growth of the minerals. The data for different silicate systems give a typical range $10^{-5} - 10^{-4}$ cm s^{-1}. The supercooling rates are estimated with the help of the adiabatic and liquidus gradients and convective velocities [*Solomatov and Stevenson*, this issue (*a*), (*b*)] as $\dot{T} \approx 10^{-4} - 10^{-3}$ K s^{-1}. The crystal radius range is estimated with the help of Figure 3 as $10^{-2} - 1$ cm.

The parameter p is in the range 10–50 and thus the mathematical procedure used is valid ($p \gg 1$). For the magma ocean range, $p = 20 - 30$, and the supercooling at which the nucleation and initial crystal growth rate occurs is about

$$T'_m = \left(\frac{A}{p}\right)^{1/2} \sim 20 \text{ K}, \tag{42}$$

and the corresponding depth interval is

$$\Delta z \approx \frac{T'_m}{d(T_{\text{ph}} - T_{\text{ad}}^{(1)})/dz} \approx 10 - 10^2 \text{ km}. \tag{43}$$

The temperature and the depth interval during which the nucleation and the initial crystal growth take place are of the order of (102)

$$T_n \sim \frac{T'_m}{p} \sim 1 \text{ K}, \tag{44}$$

$$\Delta z_n \sim \frac{\Delta z}{p} \sim 1 - 10 \text{ km}. \tag{45}$$

The standard deviation (105) for the crystal size distribution is about

$$\sigma_{\text{st}} \sim 0.1 - 0.3. \tag{46}$$

OSTWALD RIPENING

The next stage of crystal growth is Ostwald ripening. The Ostwald ripening always takes place in an equilibrium (on average) system due to the local disequilibrium for the crystals with radii smaller or larger than the average equilibrium radius [*Dunning*, 1972; *Lifshitz and Pitaevskii*, 1981]. Different kinds of Ostwald ripening act in the magma ocean. Ripening can be accomplished with the help of diffusion in the liquid or with the help of enhanced diffusion due to the relative motion between the crystals and the liquid. A specific kind of ripening can be due to convective circulation of the crystals between regions with different equilibrium crystal fraction.

The equation for the rate of crystal growth at a constant temperature is

$$\frac{dr}{dt} = G(\Delta c) = G(\Delta c_0 - \frac{\alpha_0}{r}), \tag{47}$$

where Δc_0 is the supersaturation for the zero curvature at the given temperature, and Δc is the actual supersaturation for the crystal with the radius r. The parameter α_0 is equal to

$$\alpha_0 = \frac{\sigma c_\infty v_m}{2RT} \tag{48}$$

where c_∞ is the equilibrium concentration for $r = \infty$, v_m is the molar volume, and R is the gas constant.

We note that supercooling in the multicomponent systems has the same physical nature as the supersaturation. In both cases, only the driving chemical potential difference is important. It is easy to show that for an ideal mixture the supercooling T' is connected with the supersaturation Δc as follows:

$$T' \approx T\frac{\Delta s}{R}\frac{\Delta c}{c} \tag{49}$$

provided $\Delta c \ll c$, where Δs is the entropy change on melting of the component considered, and c is the concentration of the component in the mixture. Because usually $\Delta s/R \sim 1$ we have

$$\frac{T'}{T} \sim \frac{\Delta c}{c}. \tag{50}$$

The problem of Ostwald ripening was studied for two functions of crystal growth rate $G(\Delta c)$ corresponding to the different mechanisms of crystal growth [*Greenwood*, 1956; *Wagner*, 1961; *Lifshitz and Slyozov*, 1961]:

$$G(\Delta c) = \frac{D\Delta c}{r} \tag{51}$$

if the diffusion is the rate-controlling process, and D is the coefficient of the diffusion;

$$G(\Delta c) = k\Delta c \tag{52}$$

if the interface kinetics with continuous growth mechanism is the rate-controlling process, and k is the kinetic constant. Two other mechanisms mentioned before are the screw dislocation mechanism,

$$G(\Delta c) = k_d \Delta c^2, \tag{53}$$

where k_d is a constant, and the surface nucleation mechanism,

$$G(\Delta c) = b \exp\left(-\frac{B'}{\Delta c}\right), \tag{54}$$

where b is the same constant as in (33) and

$$B' \approx \left(\frac{R}{\Delta s}\right)\frac{Bc}{T} \approx \frac{Bc}{T}. \tag{55}$$

As can be seen from the strict mathematical solutions, the asymptotic regime of Ostwald ripening can be approximately estimated for all cases with the help of the assumption that the averaged crystal radius is approximately equal to the equilibrium radius:

$$r \sim \frac{\alpha_0}{\Delta c_0} \tag{56}$$

and the changing of the averaged radius approximately obeys the equation

$$\frac{dr}{dt} \sim G(\Delta c) \sim G(\Delta c_0) \sim G(\frac{\alpha_0}{r}). \tag{57}$$

This approximation to the asymptotic solution has the same mathematical basis as in the work by *Ratke and Thieringer* [1985], who showed how to find asymptotic solutions for different problems of Ostwald ripening.

Solving this equation for the above functions of the crystal growth rate, we find

Diffusion mechanism

$$r \sim (\alpha_0 D t)^{1/3}, \tag{58}$$

Continuous growth mechanism

$$r \sim (\alpha_0 k t)^{1/2}, \tag{59}$$

Screw dislocation mechanism

$$r \sim (\alpha_0^2 k_d t)^{1/3}, \tag{60}$$

Surface nucleation mechanism

$$r \sim \frac{\alpha_0}{B'} \ln\left(\frac{B' b t}{\alpha_0}\right). \tag{61}$$

The results for the first two cases were obtained with a more accurate mathematical procedure [*Greenwood*, 1956; *Wagner*, 1961; *Lifshitz and Slyozov*, 1961].

The surface nucleation mechanism for the silicate systems is unable to provide Ostwald ripening because for typical values of $\alpha_0 \sim 10^{-7} - 10^{-8}$ cm and the residence time estimated by the convective time $t \sim 10^6$ s [*Solomatov and Stevenson*, this issue (*a*), (*b*)], the crystals can grow to

$$r \sim (10^{-5} - 10^{-4}) \ln\left(\frac{t}{10^6\ s}\right) \text{ cm}. \tag{62}$$

This means that after reaching the averaged equilibrium the local supersaturation due to the crystal curvatures is too small (it is of the order of $\alpha_0/r(0)$, corresponding to the supercooling $10^{-4} - 10^{-2}$ K) to drive the Ostwald ripening.

If other mechanisms control the crystal growth, then the crystals can grow faster. As an example, consider the case of the diffusion mechanism of crystal growth. For $D \sim 10^{-5}$ cm^{2}s^{-1} and $\alpha_0 \sim 10^{-7}$ cm

$$r \sim 10^{-2} \left(\frac{t}{10^6\ \text{s}}\right)^{1/3} \text{ cm}. \tag{63}$$

The relative motion between the crystals and the melt due to the crystal settling increases the rate of coarsing [*Ratke and Thieringer*, 1985]. For the viscosity of the melt $\eta \sim 10$ P and crystal-melt density difference $\Delta\rho/\rho \sim 0.1$, we find that

$$r \sim \left[\alpha_0 \left(\frac{D^2 g \Delta\rho}{\eta}\right)^{1/3} t\right]^{1/2} \sim 10^{-2} \left(\frac{t}{10^6\ \text{s}}\right)^{1/2} \text{ cm}. \tag{64}$$

The effect is not so pronounced at the time intervals considered.

Another effect can be due to convection which increases an effective diffusion rate [*Akaiwa et al.*, 1991]. Possibly more important is that the crystals circulate between levels having different equilibrium crystal fractions, which works as an "enforced Ostwald ripening."

When the crystals have no possibility to dissolve, as in the case of solidification of the upper mantle [*Tonks and Melosh*, 1990; *Solomatov and Stevenson*, this issue (*b*)], then the residence time is the time of crystallization (the time of disappearing of the melt phase) which provides very long ripening time scale. On the other hand, if the convection has no barriers, the crystals can very slowly circulate between the partially molten layers and completely solid deep layers, where the Ostwald ripening is slow because it is controlled by the solid state diffusion. Moreover, solid state creep maintains the crystal sizes at a recrystallization-controlled level [*Karato et al.*, 1986]. The time scale for such circulation is determined by solid state convection and in any case is much larger than the estimated time $10^3 - 10^4$ years *Solomatov and Stevenson*, this issue (*b*)]. The crystal radius reaches $1 - 10$ cm that is enough to begin settling and fractional crystallization *Solomatov and Stevenson*, this issue (*a*)].

It is interesting to estimate the crystal growth determined by the settling time, before the crystals reach the bottom and form a solid layer expelling the remaining melt. We can estimate the solution of this mathematical problem substituting the residence time $t = d/u_p \sim d\eta/r^2\Delta\rho g$, where u_p is the Stokes' velocity (assuming small Reynolds number) and $d \sim 10^7 - 10^8$ cm is the settling distance. We find that

$$r \sim \left[\alpha_0 d \left(\frac{D\eta}{\Delta\rho g}\right)^{2/3}\right]^{1/6} \sim 10^{-1} \text{ cm}. \tag{65}$$

This size does not greatly exceed the value required to begin settling, which means that growth during settling is small.

The above simple estimates show that if the Ostwald ripening is controlled by some mechanism different from surface nucleation, then the ripening can be fast and becomes essentially connected with convection and sedimentation.

DISCUSSION

Discussion of the Mathematical Solution

The problem of slow continuous phase transformations is solved analytically. The evolution of a crystallizing melt subject to adiabatic cooling, constant heat loss rate, or constant temperature drop rate passes through the following regimes: cooling in the metastable region without any nucleation and crystallization, short time interval of nucleation and initial crystallization, a transition to the asymptotic regime, and a slow quasi-equilibrium crystallization without nucleation. The first three time intervals are connected with each other as (102) $t_1 : t_2 : t_3 \approx 1 : p^{-1} : p^{-2/3}$, where p is a large parameter of the order of 20-30 found from a transcendental equation (92) or (23). This means that the nucleation occupies a short period in comparison with the metastable cooling period and produces a narrow size distribution with a characteristic standard deviation proportional to $p^{-1/2}$ (105). The duration of the last, asymptotic, regime is determined simply by the time it takes to reach the solidus in this quasi-equilibrium regime of cooling.

The problem is different from other well-studied problems such as isothermal crystallization, crystallization in initially supercooled, thermally isolated systems, and crystallization controlled by thermal diffusion and rapid quenching. The nucleation turns out to be less important for the final crystal size than in these problems, because both the characteristic nucleation rate and the time interval during which most of nucleation takes place are controlled by a competition between the cooling and crystallization. The most important (for the crystal sizes) material parameters are the growth rate function and the nucleation exponent. The dependence on other material parameters is logarithmically weak in this slow cooling limit. In some cases, however, their influence can be important and, of course, more accurate representa-

tion is possible with more experimental data. The results can be tested in numerical or laboratory experiments. At present, the agreement with some data (Figure 3) is the only support for the theory.

The analytical solution is found for any arbitrary function of crystal growth rate. This means, for example, that the experimental data can be approximated with any function which then can be used in calculations.

Which Mechanism of Crystal Growth Operates at Small Supercooling?

The crystal growth rate function is crucially important for both the initial crystallization and the subsequent Ostwald ripening. For example, if the surface nucleation mechanism would remain dominant even in the Ostwald ripening regime, the ripening would be certainly a negligible effect both in magma oceans and in all more common cases. However, it could be not the case. Most of the experiments have been done at relatively high supercooling (usually tens and hundreds of Kelvins). The nucleation and crystallization take place at $10 - 30$ K (maximum value) and the Ostwald ripening at $10^{-4} - 10^{-2}$ K. The crystal growth mechanism can be different at such small supercooling. The experimental data would be very important here.

Discrepency With the Laboratory Data

The theoretical curves and the laboratory data have a small difference in slope. It is difficult to reduce because of a weak dependence on the parameters. If it has any significance at all, we would attribute this to a simplified description of heterogeneous nucleation. Heterogeneous nucleation has a smaller energy barrier for the nucleation (we used a smaller surface tension) but also it can influence the initial conditions: the crystals can grow on preexisting impurities or on crystals of other solid phases [*Lofgren*, 1983; *Hort and Spohn*, 1991*a*]. Some low energy sites can be saturated in the very beginning of nucleation. The number of these sites does not depend on the cooling rate and thus, a weaker dependence of the crystal radius on the cooling rate could be expected. Examples of flattening of the curves are found in *Walker et al.* [1978], and *Grove* [1990], where, in some cases, crystallization started at a subcritical temperature.

Composition and Pressure Effects

The kinetics of crystal growth is influenced by composition changes, in particular, by the amount of volatiles. Water significantly decreases the peak crystal growth rate (the peak nucleation rate as well) and also decreases the peak supercooling [*Fenn*, 1977; *Swanson*, 1977; *Dowty*, 1980]. The mechanisms of this influence are not understood. It could be due to the influence of water on the surface tension, on the interdiffusion coefficients, or on the mechanism of crystal growth. *Ahrens* [1992] argues that the amount of water in a terrestrial magma ocean could be up to 1 wt.% and thus it could be an important factor which could influence the crystal sizes by 1 or more orders of magnitude.

The influence of pressure is also a poorly understood factor. Recent experiments on nucleation and crystal growth at high pressures (up to ~ 5 GPa) [*Brazhkin et al.*, 1989; 1992*a*,*b*,*c*] show that for some simple, one-component substances, the crystal sizes decrease with pressure at the same cooling rate (up to 1 order of magnitude in this pressure interval). In these experiments, the rates of supercooling are extremely high. This corresponds to a rapid cooling limit which is opposite to the slow cooling limit studied in this work. The effect observed in these experiments is explained by the dependence of the surface tension on pressure. A similar effect could work in a magma ocean, although the kinetics of phase changes for silicates at high pressures could be quite different due to the changes in the melt structure with pressure (see, e.g., recent study by *Williams and Jeanloz*, 1988). In particular, the surface tension can change significantly (due to structural changes at the molecular level) or the mechanism of crystal growth can change.

We conclude that both the water (or other volatiles) content and pressure are important factors which can influence the crystal sizes in magma oceans by 1-2 orders of magnitude in either direction. These problems again are not well studied and require further investigation.

Influence of Kinetics on Convection

We assumed that convection is not influenced by kinetics. Also we ignored the fact that turbulent convection has a wide spectrum of eddies and considered only the main flow (the largest scale). A self-consistent problem of convection with kinetics of phase changes is not a simple one. An ideal problem considered in this paper gives a basis for the study of more complicated problems of fluid dynamics of magma oceans.

CONCLUSION

1. The crystal sizes in a convective magma ocean are probably about $10^{-2} - 1$ cm after the nucleation of new solid phases and reaching an equilibrium concentration. This is close to the upper bound dividing fractional and nonfractional crystallization.

2. At least two factors can change the estimates by 1-2 orders of magnitude: water content and pressure. Both of them are poorly studied and, clearly, additional theoretical and experimental study are needed.

3. The rate of the Ostwald ripening depends on the mechanism of crystal growth at extremely low supercooling ($10^{-4} - 10^{-2}$ K). In the case of the surface nucleation mechanism, Ostwald ripening does not work on any reasonable time scale. If it is controlled by another mechanism (for example, chemical diffusion), then the crystals can grow to the critical size for suspension in the final stages of evolution of the magma ocean, when the time for the Ostwald ripening is large.

APPENDIX: ANALYTICAL SOLUTION

The equations (8) - (16) with an arbitrary function of crystal growth can be rewritten in a nondimensional form. The scales are convenient to choose at the moment when the supercooling has its maximum. This maximum will be found after the solution of the problem. The nondimensional supercooling s, radius x, and time τ are

$$s = \frac{T'}{T'_m}, \quad x = \frac{r}{r_0}, \quad \tau = \frac{t}{t_0}, \tag{66}$$

where T'_m is the maximum supercooling,

$$r_0 = \left(\frac{G_m}{J_m}\right)^{1/4}, \quad t_0 = \frac{r_0}{G_m}, \tag{67}$$

$$G_m = G(T'_m), \quad J_m = J(T'_m). \tag{68}$$

The nondimensional crystal growth rate g and nucleation rate j are

$$g = \frac{G}{G_m}, \quad j = \frac{J}{J_m} = \exp[p\lambda(s)], \tag{69}$$

where

$$p = \frac{A}{T'^2_m}, \tag{70}$$

$$\lambda(s) = 1 - s^{-2}. \tag{71}$$

At the maximum (subscript m)

$$s_m = 1, \quad \lambda_m = 0, \quad g_m = 1, \quad j_m = 1. \tag{72}$$

The nondimensional function of size distribution is

$$y(x,\tau) = f(r,t)r_0^4. \tag{73}$$

Two nondimensional constants are

$$K = \frac{4\pi\Delta H}{c_p^{(1)}T'_m}, \tag{74}$$

and

$$q = \frac{d(T_{ph} - T_{ad}^{(1)})}{dt}\frac{t_0}{T'_m}. \tag{75}$$

The equations are now written as

$$\frac{ds(\tau)}{d\tau} = -K\int_0^\infty g(s(\tau))x^2 y(x,\tau)dx + q, \tag{76}$$

$$\frac{\partial y(x,\tau)}{\partial \tau} + g(s(\tau))\frac{\partial y(x,\tau)}{\partial x} = 0, \tag{77}$$

$$g(s(\tau))y(x,\tau)|_{x=0} = \exp[p\lambda(s(\tau))], \quad \lambda(s) = 1 - s^{-2}, \tag{78}$$

$$s(\tau)|_{\tau=0} = 0, \quad y(x,\tau)|_{\tau=0} = 0. \tag{79}$$

Recently a mathematical procedure using the steepest descents method of integration was developed for the problem of crystallization in an isolated, initially supercooled system [*Buyevich and Mansurov*, 1990]. A modification of this procedure will be used to solve the problem considered. The above equations are reduced to an integro-differential equation:

$$\frac{ds(\tau)}{d\tau} = -Kg(s(\tau))\int_0^\tau X^2(v,\tau)\exp[p\lambda(s(v))]dv + q, \tag{80}$$

where

$$X = \int_v^\tau g(s(v'))dv' \tag{81}$$

The parameter p is supposed to be large, and the steepest descents method in a general form is supposed to be applied to the following integrals [*Bleistein and Handelsman*, 1975]:

$$I_1(\tau) = \int_0^\tau X^2(v,\tau)\exp[p\lambda(s(v))]dv, \tag{82}$$

$$I_2(\tau) = \int_0^\tau X(v,\tau)\exp[p\lambda(s(v))]dv, \tag{83}$$

$$I_3(\tau) = \int_0^\tau \exp[p\lambda(s(v))]dv. \tag{84}$$

At the maximum point

$$\frac{d\lambda(s(\tau))}{d\tau}|_{\tau=\tau_m} = \frac{ds(\tau)}{d\tau}|_{\tau=\tau_m} = 0 \tag{85}$$

Applying the steepest descents method several times, we find that the integrals can be related to each other and a simple algebraic system of equations is obtained:

$$KI_1(\tau_m) = q, \tag{86}$$

$$\lambda_m^{(II)} = -4KI_2(\tau_m), \tag{87}$$

$$I_2(\tau_m) = \frac{1}{p\lambda_m^{(II)}}, \tag{88}$$

$$I_1(\tau_m) = \frac{\pi^{1/2}}{2^{1/2}p^{3/2}\lambda_m^{(II)\,3/2}}, \tag{89}$$

where

$$\lambda_m^{(II)} = \left.\frac{d^2\lambda(s(\tau))}{d\tau^2}\right|_{\tau=\tau_m}. \tag{90}$$

From these equations we find

$$\frac{2^8}{\pi^2}\frac{q^4p^3}{K} = 1. \tag{91}$$

Dimensional equations have a transcendental form

$$p = \ln\left[\frac{\pi^3\Delta H a A^{3/2}G_m^3}{2^6 c_p^{(1)}\dot{T}^4 p^{9/2}}\right], \tag{92}$$

$$T'_m = \left(\frac{A}{p}\right)^{1/2}, \quad G_m = G(T'_m) \tag{93}$$

$$t_m = \frac{T'_m}{\dot{T}} \tag{94}$$

where

$$\dot{T} = \frac{d(T_{\rm ph} - T_{\rm ad}^{(1)})}{dz}v_{\rm conv} \tag{95}$$

The number of crystals after nucleation is

$$N = \int_0^\infty J(t)dt = J_m t_0 I_3(\infty) = \frac{2^4 c_p^{(1)}\dot{T}^3 p^3}{\pi^2\Delta H A G_m^3}. \tag{96}$$

The function $s(\tau)$ can also be found. When $\tau < \tau_m$,

$$s = q\tau, \quad \tau < \tau_m. \tag{97}$$

When $\tau > \tau_m$, the calculation of the integral $I_1(\tau)$ in (76) and subsequent integration of (76) results in the following simple integro-differential equation for $s(\tau)$:

$$s(\tau) = 1 + q(\tau - \tau_m) - \frac{\pi^{1/2}K^{3/4}}{3p^{1/4}}\left(\int_{\tau_m}^\tau g(s(\tau'))d\tau'\right)^3, \tag{98}$$

$$\tau > \tau_m.$$

The asymptotic solution to this equation when $\tau \to \infty$, $s \to 0$ is obtained in the form

$$g(s) = \frac{q^{1/3}p^{1/12}}{3^{2/3}\pi^{1/6}K^{1/4}\tau^{2/3}}. \tag{99}$$

There is a transition regime which is also easily described analytically. During this transition to the asymptotic regime

the crystals rapidly grow without nucleation and this transition takes the time

$$\tau_{\rm tr} \approx \tau_m p^{-2/3}. \quad (100)$$

The time interval τ_n near the maximum of $s(\tau)$ when the nucleation mostly takes place is considered in the solution as essentially small in comparison with τ_m. It is estimated from the equation $N \approx J_m t_0 \tau_n$:

$$\tau_n \approx \tau_m p^{-1}. \quad (101)$$

Thus the ratios between the time τ_m for linear increasing supercooling without crystals, the time τ_n for nucleation and initial crystal growth, and the time $\tau_{\rm tr}$ for the transition to the asymptotic regime are

$$\tau_m : \tau_n : \tau_{\rm tr} \approx 1 : \frac{1}{p} : \frac{1}{p^{2/3}} \quad (102)$$

and if $p \gg 1$, the last two time intervals are small in comparison with τ_m.

When the solid phase considered is almost crystallized and the crystal fraction of this solid phase is of the order of its maximum value ϕ_∞, the standard deviation of the crystal size distribution is estimated as follows. The variance Δx of the crystal size distribution is of the order of crystal sizes just after the nucleation:

$$\Delta x \approx g_m \tau_n = \tau_n. \quad (103)$$

Because the crystal growth rate does not depend on the crystal size, this narrowness persists in the subsequent evolution. The nondimensional crystal sizes near the complete solidification of the phase are about

$$x_\infty \approx \left(\frac{3\phi_\infty}{4\pi}\frac{J_m t_0}{N}\right)^{1/3} \approx \left(\frac{3\phi_\infty}{4\pi\tau_n}\right)^{1/3} \quad (104)$$

Thus the fractional standard deviation σ_{st} is of the order of

$$\sigma_{\rm st} \approx \frac{\Delta x}{x_\infty} \approx \left(\frac{c_p^{(1)} A^{1/2}}{\phi_0 \Delta H}\right)^{1/3} \frac{1}{p^{1/2}}, \quad (105)$$

where we used the estimate (101) and the value τ_m from the solution found.

REFERENCES

Ahrens, T. J., A magma ocean and the Earth's internal water budget, Workshop on the Physics and Chemistry of Magma Oceans from 1 bar to 4 Mbar, *LPI Tech. Rep. 92-03*, edited by C. B. Agee and J. Longhi, pp. 5-6, Lunar and Planetary Inst., Houston, Texas, 1992.

Akaiwa, N., S. C. Hardy, and P. W. Voorhees, The effects of convection on Ostwald ripening in solid-liquid mixtures, *Acta Metall. Mater., 39*, 2931-2942, 1991.

Avrami, M., Kinetics of phase changes, I, *J. Chem. Phys., 7*, 1103-1112, 1939.

Avrami, M., Kinetics of phase changes, II, *J. Chem. Phys., 8*, 212-224, 1941.

Bleistein, N., and R. A. Handelsman, *Asymptotic Expansions of Integrals*, Holt, Rinehart and Winston, New York, 1975.

Brandeis, G., and C. Jaupart, Towards scaling laws for the interpretation of igneous structures, in *Structures and Dynamics of Partially Solidified Systems, NATO ASI Ser.*, edited by D. E. Loper, pp. 329-347, Plenum, New York, 1986.

Brandeis, G., and C. Jaupart, The kinetics of nucleation and crystal growth and scaling laws for magmatic crystallization, *Contrib. Mineral. Petrol., 96*, 24-34, 1987.

Brandeis, G., C. Jaupart, and C. J. Allegre, Nucleation, crystal growth and the thermal regime of cooling magmas, *J. Geophys. Res., 89*, 10,161-10,177, 1984.

Brazhkin, V. V., V. I. Larchev, S. V. Popova, and G. G. Skrotskaya, The influence of high pressure on the disordering of the crystal structure of solids rapidly quenched from the melt, *Phys. Scripta, 39*, 338-340, 1989.

Brazhkin, V. V., S. V. Popova, and R. N. Voloshin, High pressure influence on the kinetics of solidification of the supercooled melts Pb(In), *High Pressure Res., 6*, 325-332, 1992*a*.

Brazhkin, V. V., S. V. Popova, R. N. Voloshin, L. M. Stanev, and I. G. Spirov, The kinetics of solidification of Al-Si eutectic alloys under high pressure, *High Pressure Res., 6*, 333-339, 1992*b*.

Brazhkin, V. V., S. V. Popova, R. N. Voloshin, and N. V. Kalyaeva, The influence of high pressure on the solidification of the supercooled Se melt, *High Pressure Res., 6*, 341-347, 1992*c*.

Buyevich, Yu. A., and V. V. Mansurov, Kinetics of the intermediate stage of phase transition in batch crystallization, *J. Cryst. Growth, 104*, 861-867, 1990.

Cashman, K. V., Relationship between plagioclase crystallization and cooling rate in basaltic melts, *Contrib. Mineral. Petrol.*, in press, 1993.

Christian, J. W., *The Theory of Phase Transformations in Metals and Alloys*, Pergamon, New York, 1965.

Dowty, E., Crystal growth and nucleation theory and the numerical simulation of igneous crystallization, in *Physics of Magmatic Processes*, edited by R. V. Hargraves, pp. 419-485, Princeton University Press, Princeton, N. J., 1980.

Dunning, W. J., General and theoretical introduction, in *Nucleation*, edited by A. C. Zettlemoyer, Marcel Dekker, New York, 1969.

Dunning, W. J., Ripening and ageing processes in precipitates, in *Particle Growth in Suspensions*, edited by A. L. Smith, pp. 3-29, Academic, San Diego, Calif., 1972.

Fenn, P. M., The nucleation and growth of alkali feldspars from hydrous melts, *Can. Mineral., 15*, 135-161, 1977.

Greenwood, G. W., The growth of dispersed precipitates in solutions, *Acta Metall., 4*, 243-248, 1956.

Grove, T. L., Cooling histories of Luna 24 very low Ti (VLT) ferrobasalts: An experimental study, *Proc. Lunar Planet. Sci. Conf. 9th*, 565-584, 1978.

Grove, T. L., Cooling histories of lavas from Serocki volcano, *Proc. Ocean Drilling Prog., 106/109*, 3-8, 1990.

Grove, T. L., and D. Walker, Cooling histories of Apollo 15 quartz-normative basalts, *Proc. Lunar Planet. Sci. Conf. 8th*, 1501-1520, 1977.

Hort, M., and T. Spohn, Numerical simulation of the crystallization of multicomponent melts in thin dikes or sill, 2, Effects of heterocatalytic nucleation and composition, *J. Geophys. Res., 96*, 485-499, 1991*a*.

Hort, M., and T. Spohn, Crystallization calculations for a binary melt cooling at constant rates of heat removal: Implication for the crystallization of magmatic bodies, *Earth Planet. Sci. Lett., 107*, 463-474, 1991*b*.

Huppert, H. E., and R. S. J. Sparks, Double-diffusive convection due to crystallization in magmas, *Annu. Rev. Earth Planet. Sci., 12*, 11-37, 1984.

Ikeda, Y., Grain size of plagioclase of the basaltic andesite dikes, Iritono, central Abukuma plateau, *Can. J. Earth Sci., 14*, 1860-1866, 1977.

Karato, S., M. S. Paterson, and J. D. Fitzgerald, Rheology of synthetic olivine aggregates: Influence of grain size and water, *J. Geophys. Res., 91*, 8151-8176, 1986.

Kirkpatrick, R. J., Crystal growth from the melt: A review, *Am. Mineral., 60*, 798-814, 1975.

Kirkpatrick, R. J., Kinetics of crystallization of igneous rocks, *Rev. Mineral., 8*, 321-398, 1981.

Lifshitz, I. M., and L. P. Pitaevskii, *Physical Kinetics*, Pergamon, New York, 1981.

Lifshitz, I. M., and V. V. Slyozov, The kinetics of precipitation from supersaturated solid solution, *J. Phys. Chem. Solids, 19*, 35-50, 1961.

Lofgren, G. E., Effects of heterogeneous nucleation on basaltic textures: A dynamic crystallization study, *J. Petrol., 24*, 229-255, 1983.

Lofgren, G. E., Dynamic crystallization of chondrule melts of porphyritic olivine composition: Textures experimental and natural, *Geochim. Cosmochim. Acta, 53*, 461-470, 1989.

Lofgren, G., C. H. Donaldson, R. J. Williams, O. Mullins, and T.

M. Usselman, Experimentally reproduced textures and mineral chemistry of Apollo 15 quartz-normative basalts, *Proc. Lunar Sci. Conf., 5th*, 549-567, 1974.

Marsh, B., Magmatic processes, *Rev. Geophys., 25*, 1043-1053, 1987.

Marsh, B. D., Crystal size distribution (CSD) in rocks and the kinetics and dynamics of crystallization, 1, Theory, *Contrib. Mineral. Petrol.*, 99, 277-291, 1988*a*.

Marsh, B. D., Crystal capture, sorting, and retention in convecting magma, *Geol. Soc. Am. Bull., 100*, 1720-1737, 1988*b*.

Marsh, B. D., On convective style and vigor in sheet-like magma chambers, *J. Petrol., 30*, 479-530, 1989*a*.

Marsh, B. D., Magma chambers, *Ann. Rev. Earth Planet. Sci., 17*, 439-474, 1989*b*.

Martin, D., Crystal settling and in situ crystallization in aqueous solutions and magma chambers, *Earth Planet. Sci. Lett., 96*, 336-348, 1990.

Martin, D., R. W. Griffiths, and I. H. Campbell, Compositional and thermal convection in magma chambers, *Contrib. Mineral. Petrol., 96*, 465-475, 1987.

Randolph, A. D., and M. A. Larson, *Theory of Particulate Processes*, Academic, San Diego, Calif., 1988.

Ratke, L., and W. K. Thieringer, The influence of particle motion on Ostwald ripening in liquids, *Acta Metall., 33*, 1793-1802, 1985.

Shaw, H. R., Rheology of basalt in the melting range, *J. Petrol., 10*, 510-535, 1969.

Solomatov, V. S., and D. J. Stevenson, Suspension in convective layers and style of differentiation of a terrestrial magma ocean, *J. Geophys. Res.*, this issue (*a*).

Solomatov, V. S., and D. J. Stevenson, Nonfractional crystallization of a terrestrial magma ocean, *J. Geophys. Res.*, this issue (*b*).

Sparks, R. S., H. E. Huppert, and J. S. Turner, The fuid dynamics of evolving magma chambers, *Philos. Trans. R. Soc. London, Ser. A, 310*, 511-534, 1984.

Swanson, S. E., Relation of nucleation and crystal-growth rate to the development of granitic textures, *Am. Mineral., 62*, 966-978, 1977.

Tonks, W. B., and H. J. Melosh, The physics of crystal settling and suspension in a turbulent magma ocean, in *Origin of the Earth*, edited by N. E. Newsom and J. H. Jones, pp. 151-174, Oxford University Press, New York, 1990.

Toramaru, A., Models of nucleation and growth of crystals in cooling magmas, *Contrib. Mineral. Petrol. 108*, 106-107, 1991.

Wagner, C., Theory of precipitate change by redissolution, *Z. Electrochem., 65*, 581-591, 1961.

Walker, D., M. A. Powel, G. E. Lofgren, and J. F. Hays, Dynamic crystallization of a eucritic basalt, *Proc Lunar. Sci. Conf., 9th*, 1369-1391, 1978.

Williams, Q., and R. Jeanloz, Spectroscopic evidence for pressure-induced changes in silicate glasses and melts, *Science, 239*, 902-905, 1988.

Worster, M. G., H. E. Huppert, and R. S. J. Sparks, Convection and crystallization in magma cooled from above, *Earth Planet. Sci. Lett., 101*, 78-89, 1990.

Acknowledgments. The authors wish to thank the reviewers G. Lofgren and K. V. Cashman for thoughtful criticism of the first version of the paper. Experimental data on plagioclase were substantially extended by courtesy of K. V. Cashman. This work was supported by the National Science Foundation grant EAR-89-16611.

V. S. Solomatov and D. J. Stevenson, Division of Geological and Planetary Sciences, California Institute of Technology, Pasadena, CA 91125.

(Received May 5, 1992;
revised September 9, 1992;
accepted December 4, 1992.)